DEUTSCHES ELEKTRONEN-SYNCHROTRON DESY

DESY 75/23
July 1975

Electroproduction of Neutral Pions at Energies Above the Resonance Region

by

F. W. Brasse, W. Fehrenbach, W. Flauger, J. Gayler, S. P. Goel, R. Haidan, U. Kötz, V. Korbet, D. Kreinick, J. Ludwig, J. May, M. Merkwitz, K.-H. Mess, P. Schmüser, B. H. Wiik

Deutsches Elektronen-Synchrotron DESY, Hamburg
and
II. Institut für Experimentalphysik der Universität Hamburg

2 HAMBURG 52 · NOTKESTIEG 1

To be sure that your preprints are promptly included in the
HIGH ENERGY PHYSICS INDEX ,
send them to the following address (if possible by air mail) :

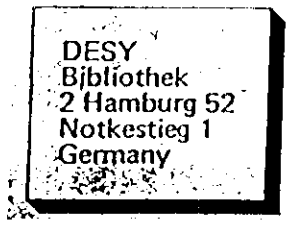

Electroproduction of Neutral Pions at Energies above the Resonance Region

F.W.Brasse, W.Fehrenbach[+], W.Flauger, J.Gayler, S.P.Goel[++], R.Haidan, U.Kötz, V.Korbel[+++], D.Kreinick, J.Ludwig, J.May[+++], M.Merkwitz, K.-H.Mess, P.Schmüser, B.H.Wiik

Deutsches Elektronen-Synchrotron DESY, Hamburg, and
II.Institut für Experimentalphysik der Universität Hamburg

Abstract:

The reaction e p → e' p π^0 has been measured at W = 2.55 GeV and a fixed electron scattering angle of 10.3 °. Two magnetic spectrometers and a lead glass hodoscope were used to detect all four final state particles. Electroproduction cross sections in the t range -0.15 to -1.4 $(GeV/c)^2$ at q^2 = -0.22, -0.55 and -0.85 $(GeV/c)^2$ are presented. Above $|t|$ = 0.6 $(GeV/c)^2$ the cross sections are considerably smaller than those for photoproduction.

+ Now at Babcock-Brown Boveri, Mannheim

++ On leave from Kurukshetra University, Kurukshetra, India

+++ Now at CERN, Geneva

The measurement of electroproduction cross sections as a function of the mass of the virtual photon can provide a stringent test for models of high energy reactions. A comparison with real photons can only be made for the transverse part of the electroproduction cross section. Charged pion production has been studied for both real and virtual photons over a wide kinematical range. In this reaction, however, the longitudinal contributions are large and no data are available for the transverse part alone. In neutral pion electroproduction the Born terms and unnatural parity exchanges and therefore the longitudinal contribution are expected to be small, so that a direct comparison between electro- and photoproduction might be attempted. Neutral pion photoproduction has been well measured, but so far no comparable data on the electroproduction have been available. In this letter we report the first data on neutral pion electroproduction above the resonance region.

In the one photon approximation the electroproduction cross section can be written [1]

$$\frac{d^4\sigma}{dE'\, d\Omega_e\, dt d\phi} = \Gamma \frac{d^2\sigma_v}{dt d\phi} \qquad (1)$$

with

$$\frac{2\pi d^2\sigma_v}{dt\, d\phi} = \frac{d\sigma_U}{dt} + \frac{d\sigma_P}{dt}\,\varepsilon \cos 2\phi + \varepsilon \frac{d\sigma_L}{dt} + \sqrt{2\varepsilon(\varepsilon+1)}\,\frac{d\sigma_I}{dt}\cos\phi \qquad (2)$$

where

$$\Gamma = \frac{\alpha}{2\pi^2}\,\frac{E'}{E}\,\frac{M^2 - W^2}{2M\, q^2}\,\frac{1}{1-\varepsilon}$$

$$W^2 = q^2 + M^2 + 2\nu M$$

$$q^2 = -4EE' \sin^2\left(\frac{\theta_e}{2}\right) = -Q^2$$

$$\nu = E - E'$$

$$\varepsilon = \left[1 + 2\,(Q^2 + \nu^2)\, Q^{-2} \tan^2\left(\frac{\theta_e}{2}\right)\right]^{-1}$$

$$\frac{d\sigma_P}{dt} = \frac{1}{2}\left(\frac{d\sigma_{\parallel}}{dt} - \frac{d\sigma_{\perp}}{dt}\right)$$

$$\frac{d\sigma_U}{dt} = \frac{1}{2}\left(\frac{d\sigma_{\parallel}}{dt} + \frac{d\sigma_{\perp}}{dt}\right)$$

ϕ is the angle between the electron scattering plane and the reaction plane

θ_e is the electron scattering angle

t is the four momentum transfer to the proton

At high energies $d\sigma_\perp/dt$ receives contributions only from natural parity [2], $d\sigma_\parallel/dt$ and $d\sigma_L/dt$ only from unnatural parity exchanges in the t-channel. Neutral pion photoproduction is strongly dominated by $d\sigma_\perp/dt$. Since pion exchange is absent the same may be expected for π^0 electroproduction. To suppress the contributions from the other terms and to maximize the data rate, we chose ϕ equal to 90° for this experiment.

For ϕ equal 90°, the interference term vanishes and $d^2\sigma_v/dtd\phi$ is a sum of positive quantities.

$$2\pi \frac{d^2\sigma_v}{dtd\phi} = \frac{(1+\varepsilon)}{2} \frac{d\sigma_\perp}{dt} + \frac{(1-\varepsilon)}{2} \frac{d\sigma_\parallel}{dt} + \varepsilon \frac{d\sigma_L}{dt} \qquad (3)$$

Thus our measurements represent an upper limit to $d\sigma_\perp/dt$ if no further assumptions are made. In this experiment ε was between 0.6 and 0.85.

The experiment was done at DESY at a center of mass energy W = 2.55 GeV. Data were taken at three values of $q^2 = -0.22$ $(GeV/c)^2$, -0.55 $(GeV/c)^2$ and -0.85 $(GeV/c)^2$ for t between -0.15 $(GeV/c)^2$ and -1.4 $(GeV/c)^2$. All four final state particles from the reaction $e\,p \to e'\,p\,\pi^0$ were observed, the charged particles with magnetic spectrometers, and the two photons from the π^0 decay in a lead glass hodoscope. The experimental layout is shown in Fig. 1.

A well defined electron beam with an energy spread of $\pm$ 0.25% and a typical intensity of 5×10^{11} electrons/sec was focussed onto a liquid hydrogen target 12 cm long. The beam intensity was measured using a secondary emission monitor (SEM) behind the target. The calibration of the SEM was frequently checked against a Faraday cup.

Beam electrons that scattered approximately 10.3° upward were detected in the electron spectrometer, which consisted of three half quadrupoles powered in series. The momentum and the angle were determined by three hodoscopes H_1, H_2 and T1. The resolution was $\pm$ 2.5 mrad in angle and $\pm$ 1.5% in momentum.

Electrons were identified using two threshold Cerenkov counters and a iron-scintillator shower counter. The solid angle $\Delta\Omega$ was 0.9 msterad; a total of 40% in momentum was accepted. For the final analysis, however, only events with a centre-of-mass energy W between 2.4 and 2.8 GeV were used.

Protons were bent vertically by a wide aperture dipole magnet. The particle trajectory was determined by three proportional chambers with a total of 2300 wires mounted at the magnet exit and a 80 x 450 cm^2 Gray code hodoscope with 450 channels, mounted about 7 m away from the target. Protons were identified by time of flight and energy loss. The acceptance in t varied between $\Delta t = 0.25$ and 0.7 $(GeV/c)^2$ depending upon q^2. The resolution in angle and momentum varied over the acceptance, but was typically $\pm$ 7.5 mrad in horizontal angle, $\pm$ 3.5 mrad in vertical angle, and 1.2% in momentum.

The lead glass hodoscope was made of a central unit of thirty-six 7 x 7 x 28 cm^3 counters surrounded by a square of sixteen 14 x 14 x 28 cm^3 counters. It was situated 3.4 m from the target, giving an angular resolution better than 20 mrad. The gain of the counters was continously monitored using light emitting diodes. The absolute energy calibration was determined by measuring elastic e p scattering, detecting electrons in the lead glass and protons with the proton spectrometer. For 3 GeV incident energy, the energy resolution (FWHM) was 11%.

All events with an e p coincidence were written on tape. π^o events were extracted by demanding two photons, each with an energy above 300 MeV, in coincidence with the scattered electron and proton. This requirement excluded Compton scattering and wide angle bremsstrahlung. The two photon effective mass distribution calculated from the measured photon angles and energies showed a very pronounced peak at the π^o mass. In Fig. 2 the time of flight spectrum for the photons measured against the scattered electron is shown. Events within a time of flight interval of $\pm$ 7.5 nsec around the peak were accepted. The small remaining background consists of accidental coincidences and events where two or more pions were produced. This background was reduced further by comparing the direction and energy of the π^o computed from the measured photons with that evaluated using the momenta and angles of the scattered electron and proton. Events where energies and angles determined by these two methods agreed within $\pm$ 17% in energy and 35 mrad in angle were accepted. It is estimated that less than 2.5% of the events were lost due to these cuts.

The distribution of the surviving events as a function of the missing mass squared computed from the scattered electron and proton is plotted in Fig. 3. A clear peak centered at a mass squared of 0.02 $(GeV/c^2)^2$ is seen. It should be noted that the acceptance limits of the spectrometer system are at $\pm$ 0.6 $(GeV/c^2)^2$. The remaining background was estimated from events where the difference in π^o angles, determined as above, was between 35 mrad and 70 mrad. This background, properly normalized, is plotted black in Fig. 3. The background was subtracted individually for each t and q^2 bin. The data were corrected for radiative effects; the correction varied between +5% and 18%. Further corrections were made for counter inefficiencies (1.03 $\pm$ 0.02) and deadtime (1.09 to 1.14 $\pm$ 0.04). Further systematic errors come from the acceptance calculations, the reproducibility of the detector and the measurement of the beam intensity. From all these effects we estimate a total systematic uncertainty of 10%.

We have evaluated a cross section $2\pi\frac{d^2\sigma_V}{dt\ d\Phi}$ at $\Phi = 90^o$. For comparison with the photoproduction data we have plotted $\frac{2}{1+\varepsilon}\ 2\pi\frac{d\sigma_V}{dt\ d\Phi}$ as a function of t in Fig. 4. This cross section (Eq. 3) represents an upper limit to $d\sigma_\perp/dt$ and is equal to $d\sigma_\perp/dt$ if $d\sigma_\parallel/dt$ and $d\sigma_L/dt$ are negligible. The photoproduction cross section for photons polarized normal to the production plane, shown as the solid line in Fig. 4, was obtained by combining cross section data[3] at W = 2.88 GeV with the available data on the photon asymmetry[4]. The cross section so derived was extrapolated to W = 2.55 GeV using the effective trajectory[4] $\alpha(t) = 0.19 + 0.27 \cdot t$. For small $|t|$, the electroproduction cross section falls exponentially, however note that the slope is less than the slope observed in the photoproduction data. In contrast to photoproduction the electroproduction cross section continues to decrease exponentially to t = -.9 $(GeV/c)^2$, and there it flattens out rather than forming a second maximum. Between $q^2 = -0.22$ and $q^2 = -0.85$ $(GeV/c)^2$ the size of the cross section for large values of t varies little compared to the factor of 9 change between $q^2 = 0$ and $q^2 = -0.22$ $(GeV/c)^2$. Since in this experiment only an upper limit to $d\sigma_\perp/dt$ is determined, a possible dip in $d\sigma_\perp/dt$ might have been washed out by contributions from $d\sigma_\parallel/dt$ and $d\sigma_L/dt$. At small and fixed $|t|$-values the cross section varies roughly as the first power of the ρ-propagator. At large values of $|t|$ the cross section decreases only slowly with q^2 beyond $q^2 = -.22$ $(GeV/c)^2$.

Harari[5] has suggested that a comparison of π^o photo- and electroproduction

could in principle distinguish between the various proposed dip mechanisms. It seems difficult to reconcile the present data with a weak absorption model where the dip is caused by a wrong signature nonsense zero. A strong absorption or dual absorption model might be able to fit the data. However, even in such a model the rapid decrease in cross section from $q^2 = 0$ to $q^2 = -0.22$ (GeV/c)^2, and the slow variation above -0.22 (GeV/c)^2 is surprising.

Acknowledgement:

We wish to acknowledge the invaluable support of our technicians and the DESY Hallendienst.

Figure Captions:

1) Experimental Layout.

2) The difference of electron and photon flight times for e p γ γ events. The zero of the time scale is arbitrary.

3) Number of events surviving all e' p π^o cuts as a function of missing mass squared computed from the electron and the proton. The background estimate (see text) is shown in black.

4) The cross section $\frac{2}{1+\varepsilon} 2\pi \frac{d^2\sigma_V}{dt\, d\Phi}$ for $ep \to e'p\pi^o$ at $\Phi = 90^o$ is plotted as a function of t for various values of q^2.
The cross section $d\sigma_\perp/dt$ for real photons is shown as the solid line.

References:

1) K. Berkelman, Proc. of the International Symposium on Electron and Photon Interactions at High Energies, Hamburg 1965
and
M. Gourdin Nuovo Cimento 21, 1094 (1961)

2) G. Kramer Acta Physica Austriaca 40, 150-157 (1974)

3) P.S.L.Booth et al., Annual Report 1972 Daresbury Nuclear Physics Lab.
and
J.R. Holt, Private communication

4) B.H. Wiik, Proc. of the International Symposium on Electron and Photon Interactions at High Energies, Cornell University, Ithaca, 1971

5) H. Harari, Phys. Rev. Letters 27 (1028) 1971

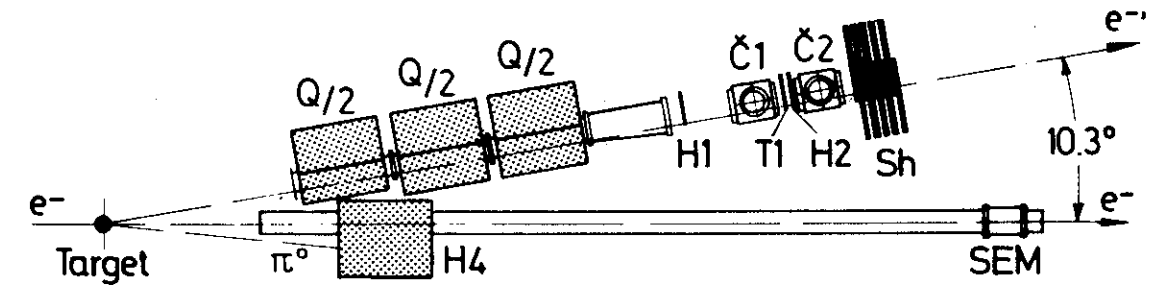

SIDE VIEW
of e^- and γ-Detector

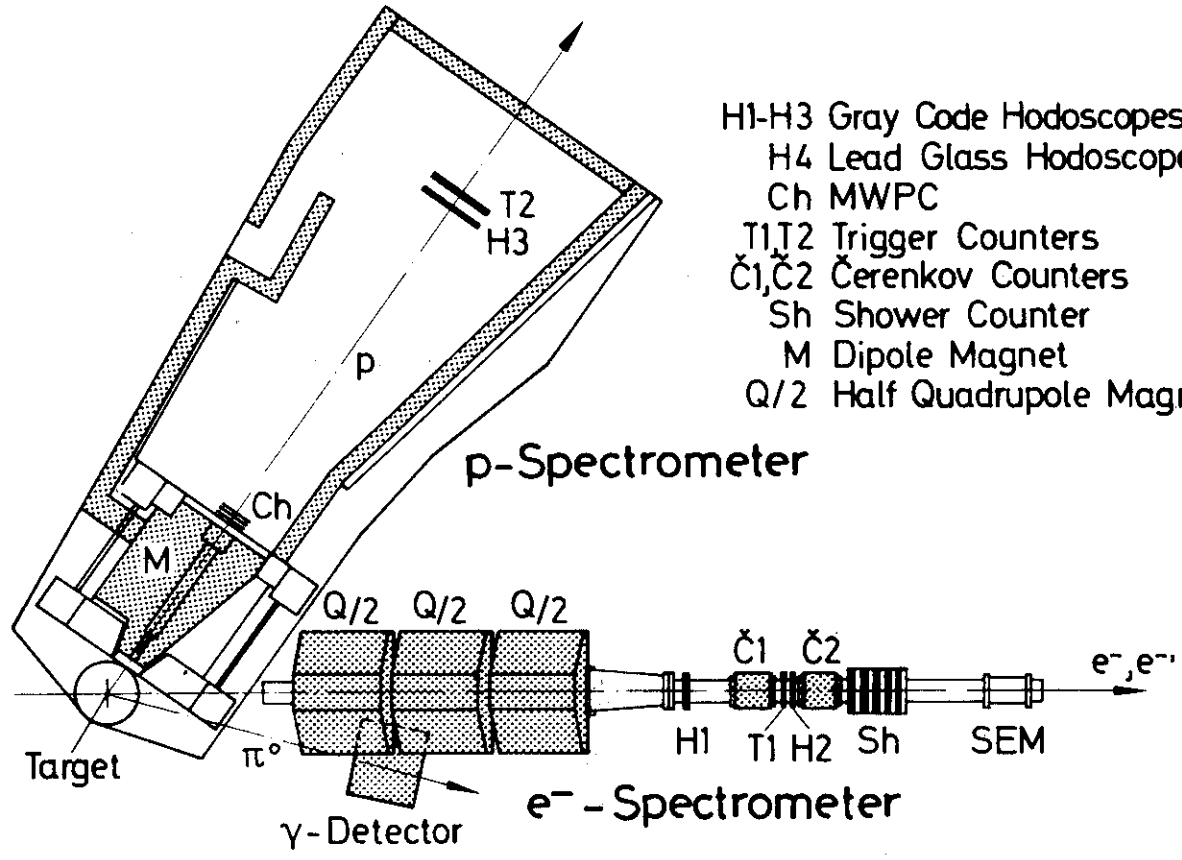

H1-H3 Gray Code Hodoscopes
H4 Lead Glass Hodoscope
Ch MWPC
T1,T2 Trigger Counters
Č1,Č2 Čerenkov Counters
Sh Shower Counter
M Dipole Magnet
Q/2 Half Quadrupole Magnets

TOP VIEW

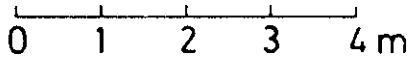

Fig. 1

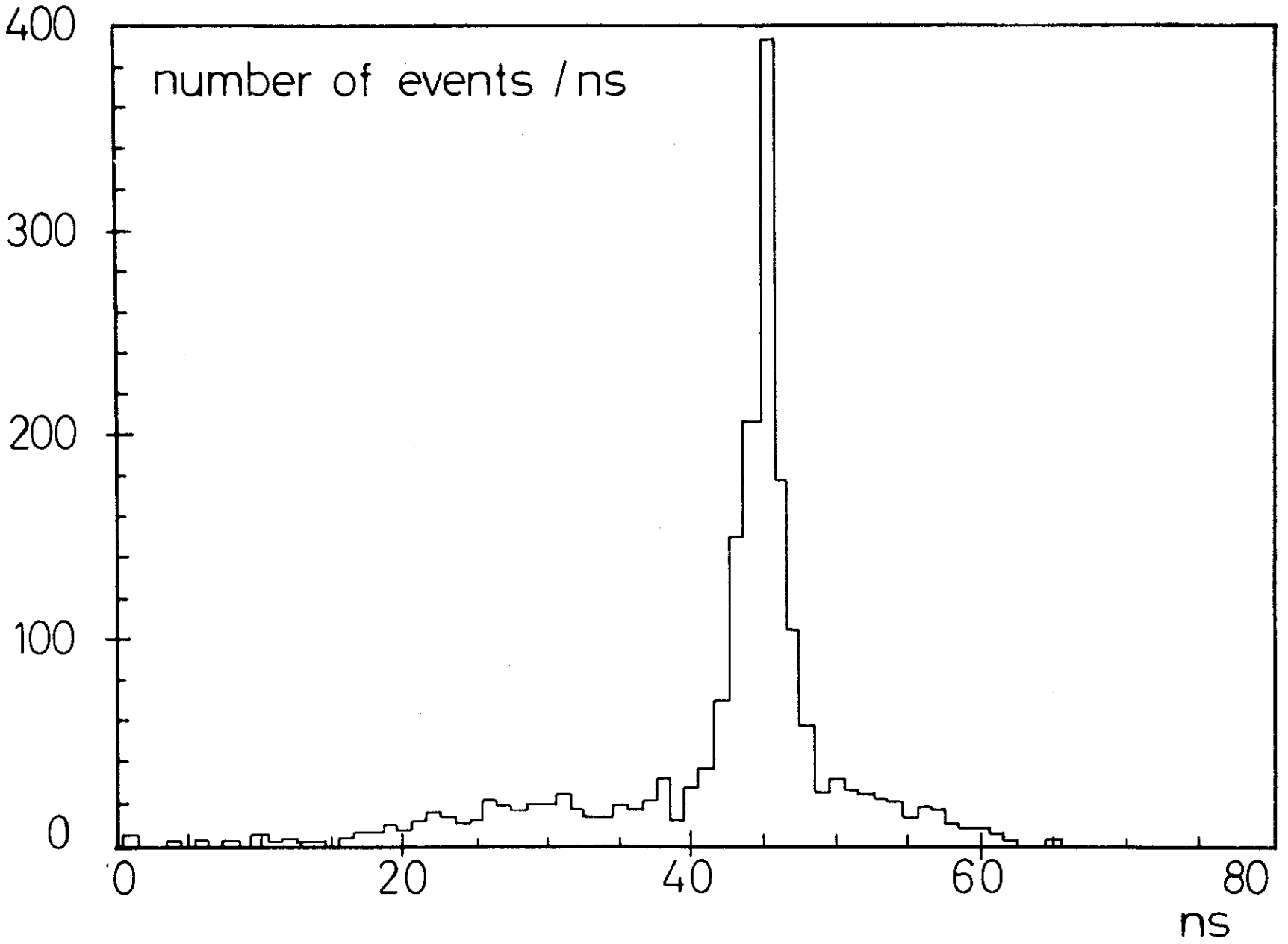

Fig. 2

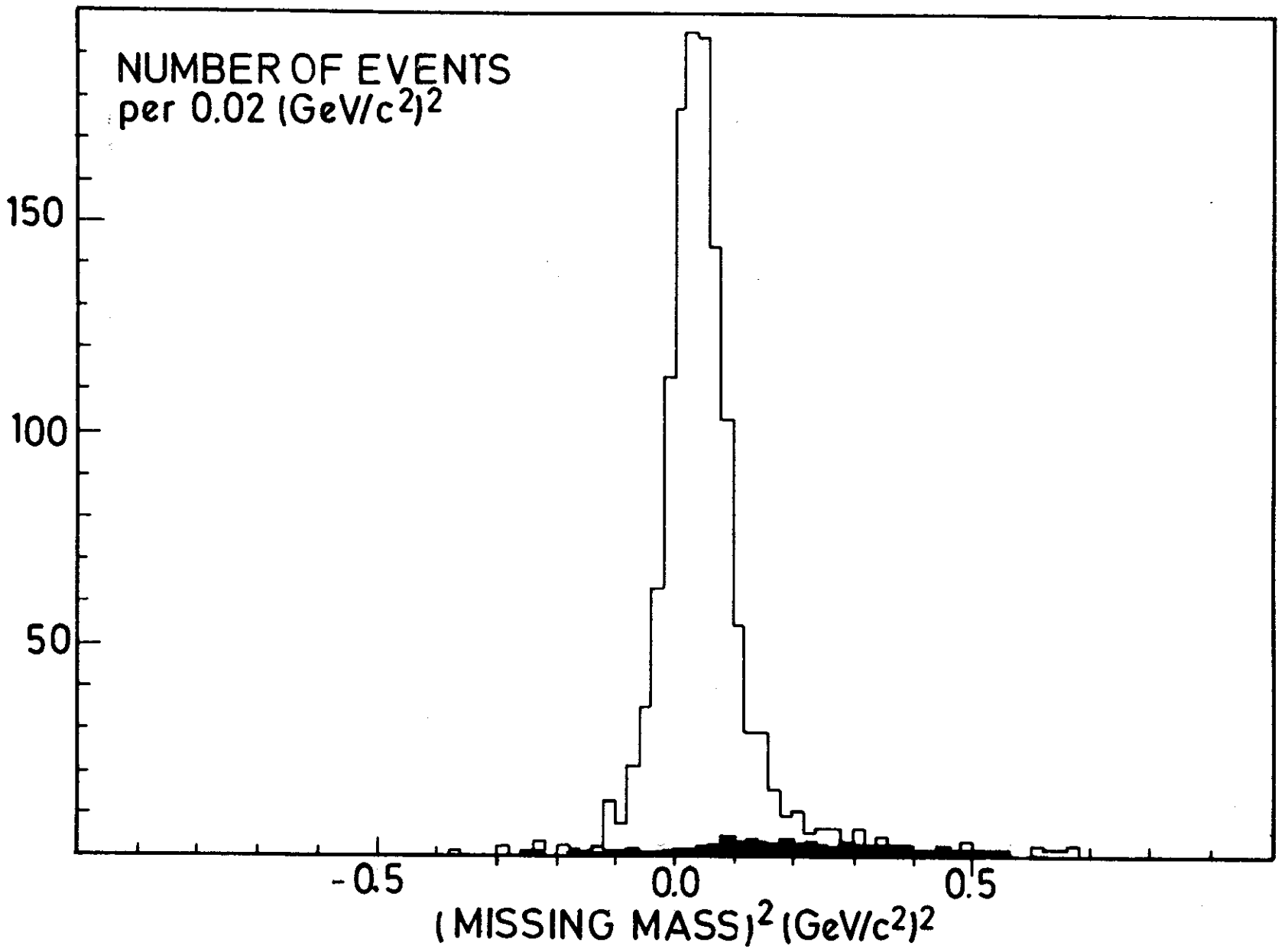
NUMBER OF EVENTS
per 0.02 (GeV/c²)²
150
100
50
-0.5
0.0
0.5
(MISSING MASS)² (GeV/c²)²

Fig.3

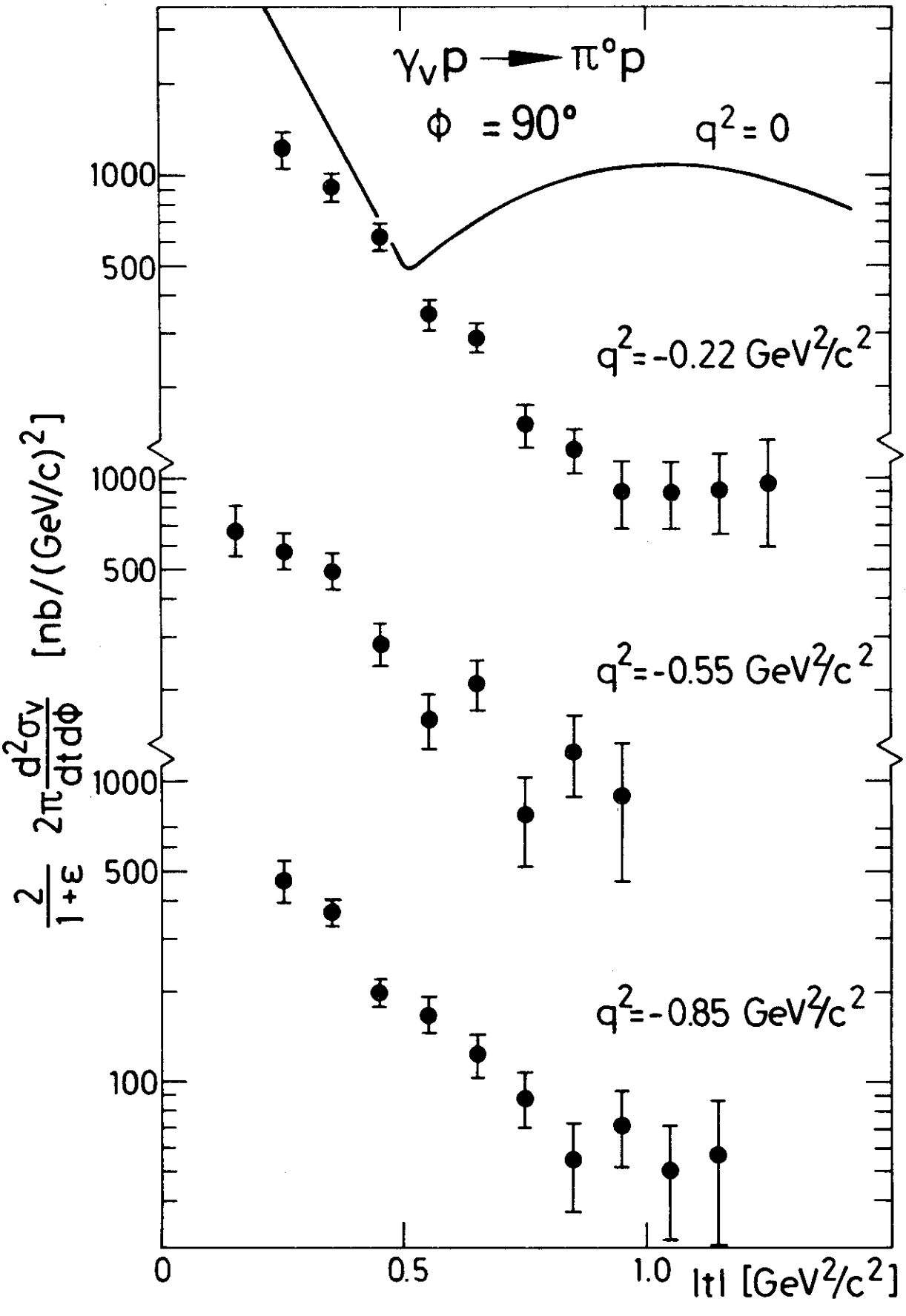
$\gamma_v p \rightarrow \pi^0 p$
$\phi = 90°$
$q^2 = 0$
$q^2 = -0.22\ GeV^2/c^2$
$q^2 = -0.55\ GeV^2/c^2$
$q^2 = -0.85\ GeV^2/c^2$
$\frac{2}{1+\varepsilon} 2\pi \frac{d^2\sigma_v}{dt\,d\phi}$ [nb/(GeV/c)^2]
1000
500
1000
500
1000
500
100
0
0.5
1.0
|t| [GeV^2/c^2]

Fig. 4